

INTERRELATION BETWEEN GRIT MORPHOLOGY AND DEFIBRATION PERFORMANCE IN PRESSURIZED GROUNDWOOD PROCESS

Authors*: Olli Tuovinen¹
Pedro Fardim²

ABSTRACT

This investigation is one in the series of studies involving the performance of grinding process, morphological characteristics of grinding grits and topographical features of grinding surfaces. This paper introduces results of interrelation between grit morphology and grinding performance in pressurized groundwood process. These lab scale studies were done with single layer grinding surfaces using different aluminum oxide grits as grinding media. Results are compared to the performance of conventional vitrified ceramic pulp stone made with fused aluminum oxide grits. Results showed clearly that the energy performance of groundwood process could be improved by improving grit morphology on single layer grinding surfaces. The information of these studies has already been used in development of a new kind of grinding technology based on single layer grinding surface for mechanical pulp manufacturing. This new technology is called Galileo grinding technology.

INTRODUCTION

Wood defibration in groundwood process is based on mechanical interaction between wood and grinding grits of the pulp stone surface. Since the 1930s, pulp stone technology has been based on vitrified ceramic construction and fused corundum grits. Since then very little development has taken place in the basic materials and basic construction of pulp stones. The major changes have been the increase of unit capacity of grinders, which has made the grinder stone larger in size.

Energy efficiency of mechanical pulping, including groundwood pulping processes has been extensively studied during recent years [1-8]. Some of this research has indicated that the design of pulp stone plays a central role in groundwood process energy efficiency. Papers and patents have been released with results of trials using single layer grinding tools. These tools have been proposed as

potential alternatives for vitrified ceramic construction [3,9-10]. Some papers have brought out the importance of grit quality as well [11-13]. So far, no quantitative data has been published on the interrelations between grit morphological characteristics and performance of single layer defibration tools.

According to existing knowledge, the root cause for high-energy consumption of conventional pulp stone can be derived from its 3D construction and its impact on grinding intensity distribution [9-10]. Despite its defined grit size, the actual imprint size of grit that is in contact with wood fibers is varying a lot. The 3D construction and wear of the corundum grit leads to a situation where the grits in the wood interface can be anything between a pointed grit edge and a half of grit. A typical topography of vitrified pulp stone surface is seen in **Figure 1**. For groundwood production this kind of defibration surface is not ideal for several reasons.

Because of the 3D construction of conventional pulp stone ceramics, the grits are on different level in respect to wood and thus they expose defibration pulses with varying intensities. Some of the pulses are weak and are only absorbed in the wood and transferred into heat. Some of the pulses are large and may overcome the strength of the fibers and thus cause damage to wood resulting in cut fibers, release of fiber bundles (shives) and fibers with low internal fibrillation.

In a worn surface of vitrified pulp stone, half of the grits act like large grits with small rake angle and they expose large defibration pulses but with low intensity into the wood. These kinds of defibration pulses are quite inefficient and are absorbed in the wood and transformed into heat without significant structural damages. The grits deeper in the vitrified pulp stone structure but in the defibration plane have pointed edges with a large rake angle. These grits expose localized defibration pulsed with high intensity. These pulses are bound to cut fibers.

* Authors references:

1. M.Sc., Valmet Technologies Oy, Finland, FIN-33101 Tampere, Finland. E-mail: olli.tuovinen@valmet.com
2. Professor, Åbo Akademi University, FIN-20500 Åbo, Tampere, Finland. E-mail: pfardim@abo.fi

Corresponding author:

Olli Tuovinen - Valmet Technologies Oy, Finland, FIN-33101 Tampere, Finland. E-mail: olli.tuovinen@valmet.com

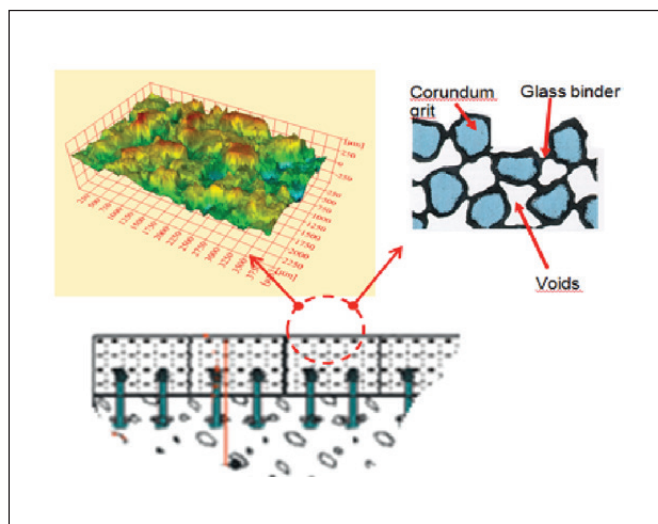


Figure 1. Construction of vitrified grinding surface

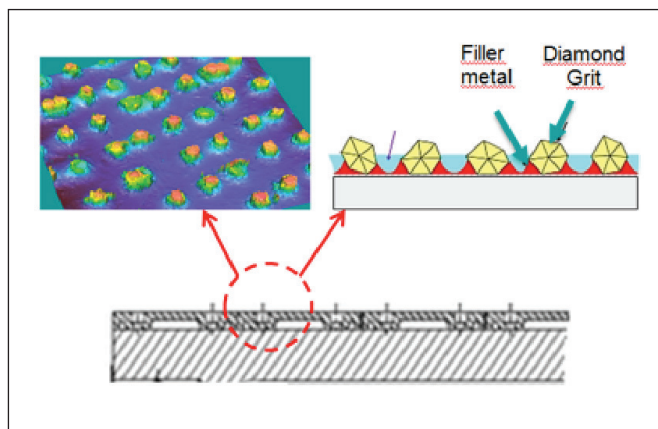


Figure 2. Construction of single layer coated grinding surface

Grinding grits are randomly distributed in the 3D construction of vitrified pulp stone also in the 2D plane, which is in contact with the wood. Therefore, the fibers become treated unevenly before they are released from the wood. The energy consumption increases because repeated uncontrolled loading of same locations of fibers.

Increasing the wood-feed rate and grinding pressure with such a surface increases predominantly the intensity of large grits causing additional heating of wood and therefore an increase in Canadian Standard Freeness (CSF). This limits the possibilities of increasing the grinder production rate and reducing energy consumption without increasing CSF at the same time.

This paper introduces lab scale research results along the path towards a new grinding technology (Galileo). The main focus of this paper is the development of grit morphology and how this development influences energy consumption and the pulp quality of the grinding process. The studies were done on single layer grinding surface using various aluminum oxide grits. Synthetic diamonds were also analyzed for their morphology as reference materials.

MATERIALS AND METHODS

Grit material and its treatments

The quality of aluminum oxide grits were the focus in the first step towards developing improved grinding surfaces. After considering various commercial grits, the Treibacher (Imerys) SCT Mesh #60/70 fused grit was chosen as the starting point for further development of grit morphology. The basis of the selection was that the natural form of this mono-crystalline alumina grit is very regular and blocky already after fusing and crushing. The difference between normal fused and crushed alumina grits can be seen in **Figures 3a** and **b**. Standard FEPA-F sieve analysis result of SCT Mesh #60/70 grit used in this test is listed in **Table 1**.

The morphological characteristics of these standard SCT grits were developed further by sieving them according to their size and shape. First the SCT grits were classified by size into so-called nominal grain, which is the major sieve fraction (S3+S4). This fraction was about 77% of the sieving feed material.

Shape development was done by using tilted vibratory table, which classified the grit material into 10 classes. This classification is based on flowing characteristics of the grits. Roundish particles flow

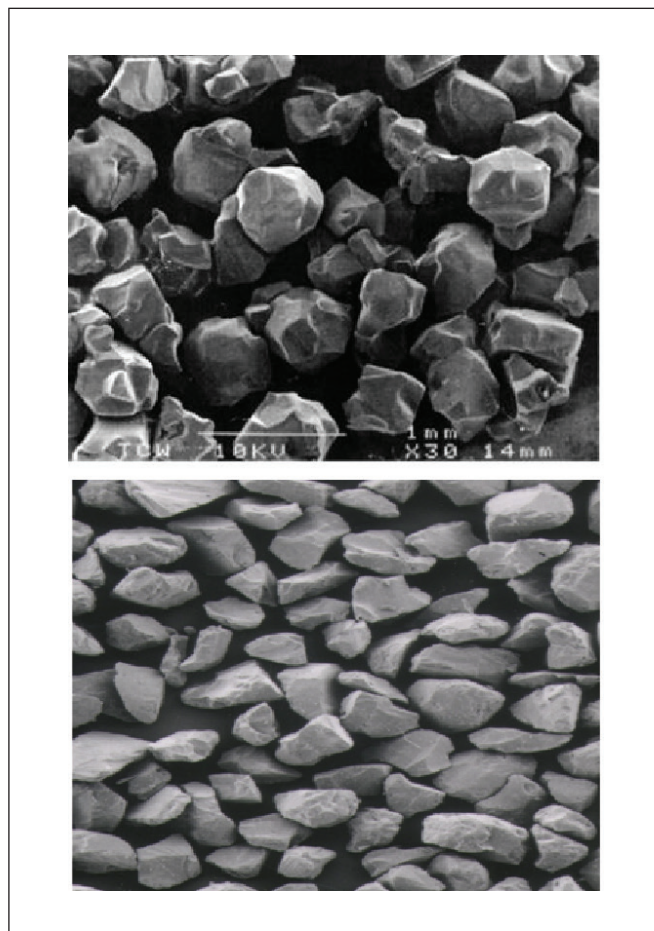


Figure 3a. Fused single-crystal Treibacher (SCT) alumina grits and Figure 3b fused (conventional) alumina grits, (SEM images published with permission from Treibacher (Imerys))

TABLE 1. STANDARD FEPA-F SIEVE ANALYSIS OF TREIBACHER #60 MESH SCT ALUMINUM OXIDE GRITS

Size (mm)	S1 +0.425	S2 +0.300	S3 +0.250	S4 +0.212	S5 +0180	-0.180	Bulk density g/cm ³
Tolerance, w-%	0	0-30	40-100	65-100	0-35	0-3	1.77-1.87
Sample, w-%	0	21	60	77	2	0	1.78

Note: On sieve S4 = S3+S4.

more directly to the outflow ports (F7-F10) whereas more extended, angular and pointed particles flow more towards the tilted direction of the table before entering to the outflow ports (F1-F4). Tilt angle of the table was adjusted so that the major part of the flow was directed to the center of the 10 classification ports but also so that ports 1 and 10 received some of the flow. The results of shape classification are in **Table 2**. Already the bulk density analysis revealed that shape classification took place.

The amount of material to the ports F1, F2 and F10 was so small that bulk density measurement could not be done.

The size and shape factors of the grits were also measured using microscope and image analysis tools. Before analyses, the AI system was scale calibrated using 1mm /0.01 mm calibration graticule.

Sample preparation for IA was done as follows. Transparent sample beds were made on glass Petri dishes. The beds were prepared by melting one teaspoon of Agar powder into 100 mL 95°C tempered distilled water. After melting and mixing, the melt was poured as an even thin layer on the Petri dishes and left to gel. After the Agar had formed a gel, a small amount of grits was sprinkled over the Agar gel. The grits stuck and sunk marginally into the Agar gel bed. Then the Agar was cooled further until a firm gel bed was created. Use of this Agar gel method was

Table 2. Fraction shares and bulk densities of fractionated sct #60 mesh aluminum oxide grits

Fractions	Share W-%	Bulk density g/cm ³
Base material	100	1,74
Nominal fraction	77	1,73
F1	1	-
F2	2	-
F3	2	1,41
F4	10	1,54
F5	17	1,67
F6	24	1,78
F7	21	1,89
F8	15	1,99
F9	7	2,06
F10	1	-

Table 3. Main data of ai system used for grit analyses

Microscope	Olympus BH-2
Illumination	Microscope lamp, pass-through light arrangement, polarization filter
Digital camera	SIS Color-Wiew12, 1280 x 1024, 3 x 12 bit
Frame grabber	SIS GarabBit
IA software	AnalySiS Pro
Calibration graticule	Pyser Graticules, P58, 1mm/0.01 mm

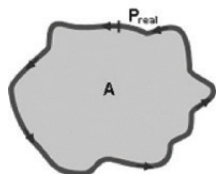
found necessary to diminish the effect of grit shape in sample preparation and analysis results.

Samples were then analyzed under the microscope. Arrangement (**Table 3**) allowed analyzing max 5 grits in one view. Theoretical pixel resolution was about 2 µm. Optical resolution was considered to be enough for this pixel resolution. The G (green) channels of the RGB camera were used to create the 12 bit grayscale images. The image contrast was improved by using polarization filter both in front of the microscope light and in front of the microscope objective. The polarization planes of the filters were in 90-degree angle with respect each other. Without sample, the microscope field was completely black. The crystalline translucent grits turned the polarization plane of the light and therefore the grits themselves could be seen as bright objects in the microscope field. The Petri dish was moved by microscope X-Y table and the multitude of grits images were taken for further morphological analyses.

It was in our interest to analyze the particles for their **roundness** and **roughness**. "Roundness" was calculated as "**sphericity**" and "roughness" was calculated as "**convexity**". At this point it is worth mentioning that "roundness" and "roughness" cannot be considered as totally independent parameters.

Sphericity [14]

The sphericity, S , is the ratio of the perimeter of the equivalent circle, PEQPC, to the real perimeter, P_{real} .



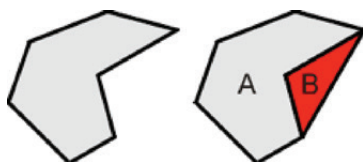
The sphericity is defined by the formula:

$$S = \frac{P_{EQPC}}{P_{real}} = \frac{2\sqrt{\pi \cdot A}}{P_{real}}$$

The result is a value between 0 and 1. The smaller the value, the more irregular is the shape of the particle. This results from the fact that an irregular shape causes an increase of the perimeter. The ratio is always based on the perimeter of the equivalent circle because this is the smallest possible perimeter with a given projection area.

Convexity [14]

The convexity is a shape parameter describing the compactness of a particle. The figure shows a particle with projection area A (grey/light) leaving open a concave region of area B (red/dark) on its right hand side.



The convexity is defined with the formula:

$$\psi_c = \frac{A}{A+B} = 1 - \frac{B}{A+B}$$

Sample size determination

Sampling and analysis of grits may be challenging and care must be taken that enough material is to be analyzed to enable a representative value for morphological figures. In this case we made three individual samplings from the grit material on the Petri dishes. Analysis of grits in each Petri dish was continued until we reached a "good average number" for measured parameters.

Evaluation of this criterion was done by calculating a running average and a running differential of the running average for each dish. Analysis of grit results was continued until the differential

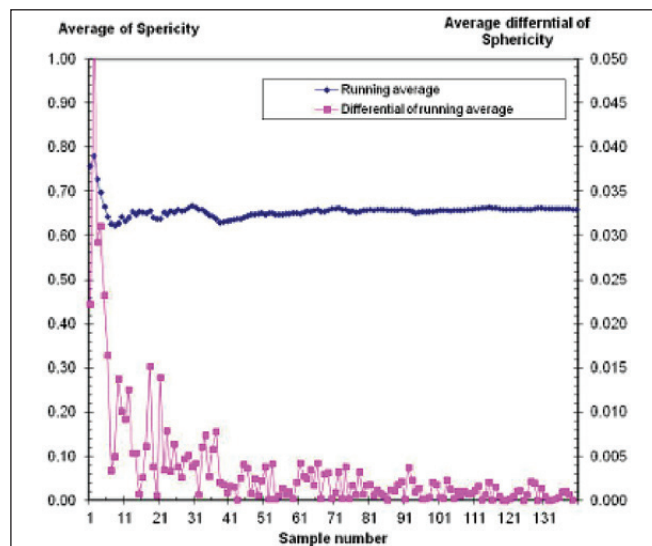


Figure 4. Running average and differential of running average of grit sphericity for sample size determination

of successive numbers of the running average reached a level less than 2‰ (Figure 4). After this, the results of all three-sample populations were combined and finally a combined average numbers of morphological parameters were calculated.

Laboratory grinding trials

Laboratory trials were done with Spruce from Southwestern Finland. The wood was debarked and cut in 40 mm slices. These wood slices were further cut to wood sticks of 38-40 mm in width. Between different trials the unused wood sticks were stored in a freezer.

Trials with aluminum oxide grits were done with a laboratory scale grinder at Åbo Akademi University, Turku, Finland. The main parameters of this grinder are listed in Table 4.

About 400 g of wood were ground using 1.0 – 2.0 mm/s shoe speeds for each point. The pulp was ground to a pressure vessel. During the trials, all the essential process parameters were logged and stored for further analyses. Production calculation was based on pulp volume and its consistency during each sample point. Specific energy consumption of each sample was calculated from the cumulated energy and said production.

After the trials each sample was prescreened by vibratory

Table 4. Main parameters of laboratory scale grinder in Åbo Akademi University

Max grinding power	MW/m ²	2.5
Max grinding pressure (wood pressure)	bar	10
Max grinding speed	mm/s	2.5
Max casing pressure	bar	4.5

Table 5. Main parameters of laboratory scale grinding surfaces

Diameter of grinding wheel	mm	300
Width of the grinding wheel	mm	50
Size of segments	mm x mm	50 x 50
Number of segments	pc	18
Type of grit		SCT
Grit population density	Pc/cm ²	125
Grit diameter	Mesh	60/65

screen made with 6 mm holes. The reject amount was kept to minimum so that all large shives could be removed, but fiber loss was kept small. After this, the pulps were analyzed using ISO standard methods for pulp and paper.

Grinding surfaces for lab studies

The choice of production parameters of lab surfaces was done so that we could test the hypothesis that a smooth grinding surface, which is made with grits of least variation in size and shape, would provide a good standpoint for improving the performance of the grinding surface. The performance of these surfaces was assessed by their energy efficiency, pulp quality and production rate. A standard Mesh 60 grits pulp stone was used for production of reference pulps.

The main parameters of the tested Galileo surfaces are listed in **Table 5**. Single layer grinding tools were produced on steel segment bodies for these trials. Grit population density could be controlled using special production methods. The grits were fixed on the steel segment bodies by a brazing method in high vacuum and in high temperature furnace ($T > 1000^{\circ}\text{C}$). Incusil ABA was used as the braze.

Two coated surfaces were produced, one with standard SCT grit (**A_surface**) and the other with improved SCT grits, SCT_F9 (**M_surface**). SCT_F9 is the F9 fraction of shape classification. The share of this fraction was 5.4 m-% of the original SCT grit sample.

RESULTS AND DISCUSSION

Grit morphology

Figure 5 illustrates the development path of SCT aloxy grits for their sphericity and convexity. Aloy grits of conventional pulp stones and industrial diamonds are shown as reference materials. As can be noted, the grits of conventional pulp stone are at the same level in sphericity, but their convexity number is marginally higher than

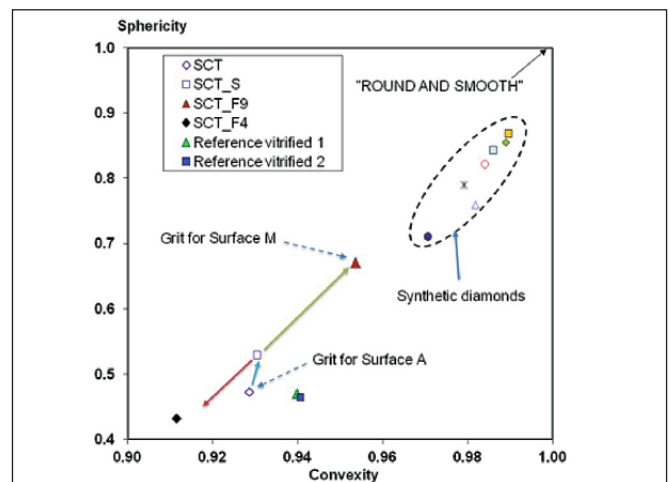


Figure 5. Sphericity versus convexity of various grit and diamond samples analyzed for the tests

that of basic SCT grits. After sieving by size and shape, the SCT_F9 grits were superior in convexity and sphericity in comparison to the conventional pulp stone grits

Compared to synthetic industrial diamonds, even the improved SCT_F9 grit was at a lower level as regards the measured morphological characters. It is noticeable that even among synthetic diamonds these morphological characters varied significantly. The lower quality numbers of diamonds were at the level of improved SCT_F9 grit, whereas the highest quality numbers of diamonds exceeded the sphericity of improved SCT_F9 grits by 26%. Also as regards convexity, the difference between SCT_F9 grit and industrial diamonds was noticeable.

Lab grinding trials

Figure 6 illustrates CSF development in relation to shoe speed for lab surfaces. The coated A_surface with standard SCT had an even steeper response to shoe speed than the reference stone. M_surface had the

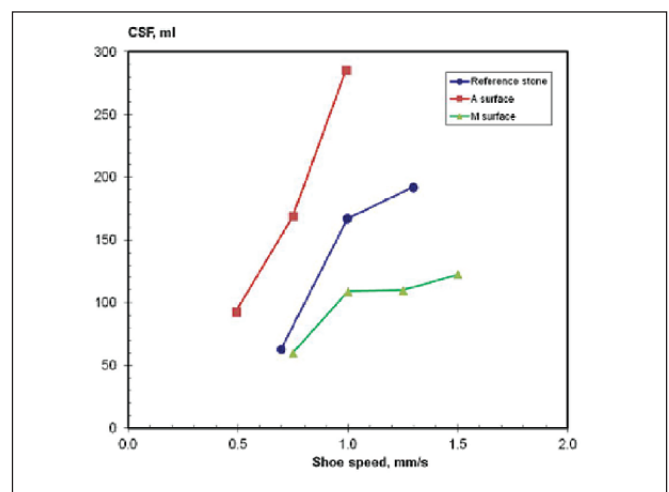


Figure 6. CSF versus shoe speed for tested lab surfaces (lines added to guide the eyes)

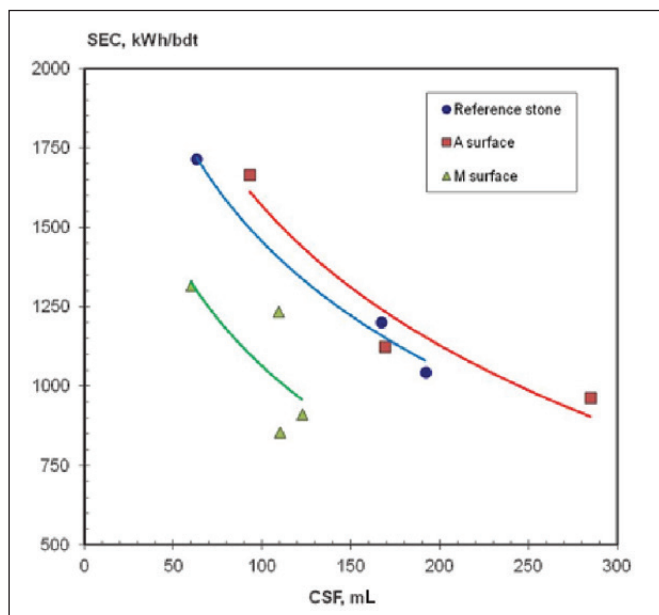


Figure 7. SEC versus CSF for various lab surfaces

desired performance in this respect and its CSF response for increased shoe speed remained significantly milder than that of the reference.

Partially because of the mild CSF response to increased shoe speed, the specific energy consumption of M_surface was also significantly lower than the reference. A comparison at the 100 mL CSF level, A_surface and the reference were at the same level – 1500 kWh/bdt, which is typical for PGW70 made from spruce at this CSF level. The Surface M, on the other hand, was much lower – 1050 kWh/bdt in SEC (Figure 7).

Pulps from M_surface and the reference performed equally when compared for their tensile indexes at CSF level 100 mL. Pulp from A_surface had lower tensile in same CSF (Figure 8) than the other pulps.

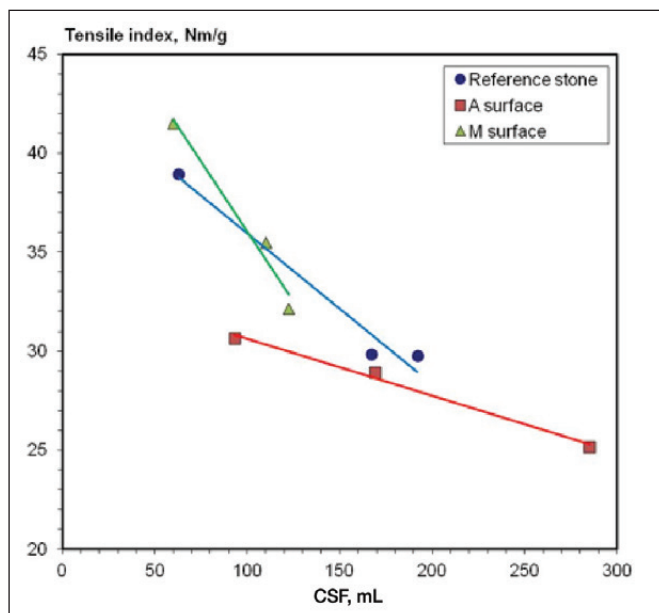


Figure 8. Tensile index versus CSF for various lab surfaces

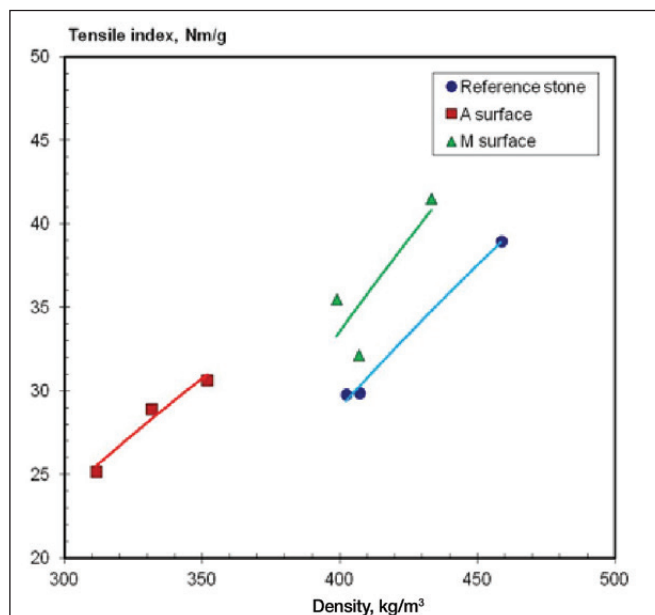


Figure 9. Tensile index versus apparent sheet density for various lab surfaces

Both the reference and M_surface pulps were at the same density level, but A_surface pulp was significantly bulkier. The tensile to density ratio appeared to be similar for both coated surfaces, whereas the tensile level of the reference surface appeared to be lower if comparison is made of the same density (Figure 9).

Tear index was similar for the reference and M_surface pulps. A_surface pulp was somewhat higher in tear (Figure 10).

At a constant tensile level, the light scattering coefficient of A_surface pulp appeared to be superior to the reference stone pulp. On the other hand, M_Surface pulp LSC was about 2%-3% points lower than the reference (Figure 11).

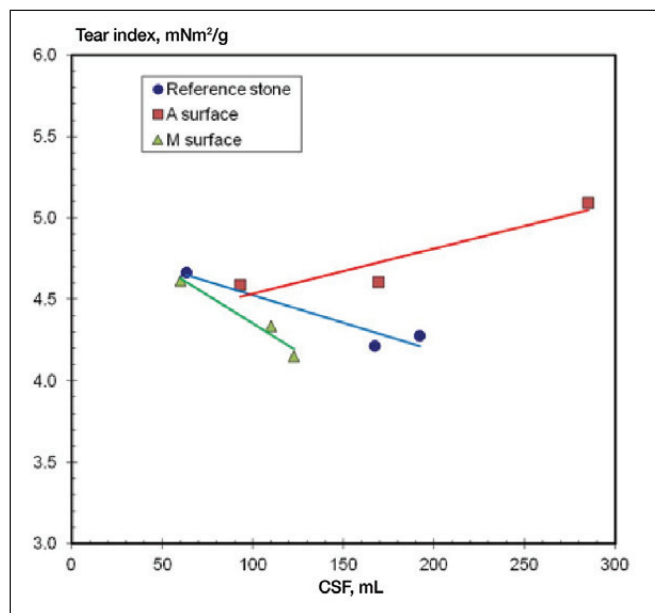


Figure 10. Tear index versus CSF for various lab surfaces

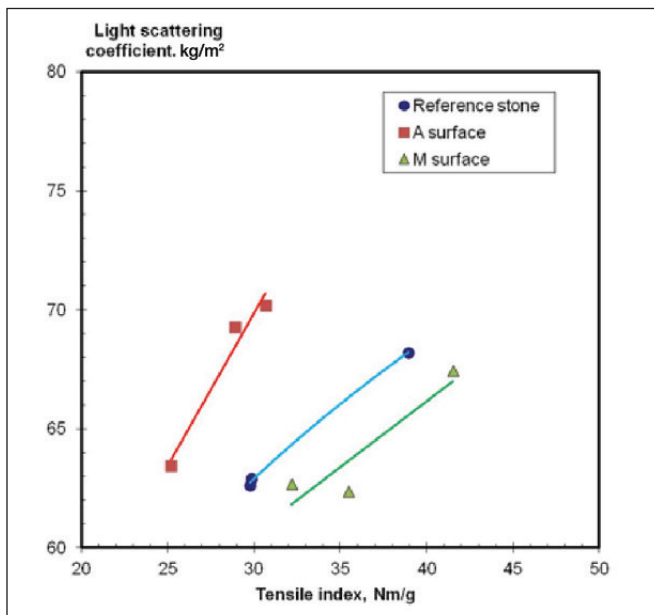


Figure 11. Light scattering coefficient versus tensile index for various lab surface

CONCLUSIONS

The trial results revealed a clear correlation between grit

morphology and performance of grinding surfaces. The results have enhanced our understanding of the reasons for basic differences in performance of traditional 3D pulp stones and single layer (2D) grinding surfaces. Furthermore, these results have made it possible to enhance the performance of single layer grinding tools by applying the new knowledge of the interrelation between grit morphology and the defibration and energy performance of single-layer grinding surfaces.

Even if the results of these lab studies can be considered excellent, the use of aluminum oxide grits as raw material for any practical single layer grinding tools for groundwood production is not realistic. In order to make mill-scale surfaces with long life expectancy, super abrasives like synthetic diamonds need to be used. As shown in this paper, synthetic diamonds are available in a broad range of quality. In morphological characters they are even better than the best aluminum oxide grits developed in the present study.

This background provides good opportunity for developing new kinds of grinding tools, which can improve energy efficiency of existing commercial GW and PGW grinders.

The authors wish to share further results from the Galileo development path, which will include pilot-scale and mill-scale studies in the upcoming papers. ■

REFERENCES

- Björkqvist, T., *A Design Method for an Efficient Fatigue Process in Wood Grinding - an Analytical Approach*, Doctoral Thesis, 2002, Tampere University of Technology: Tampere, p. 104
- Björkqvist, T., Lucander, M., *Grinding surface with an energy efficient profile*, 2001 International Mechanical Pulping Conference, Helsinki, Finland June 4 - 8 2001, Proceedings volume 2, p. 373 - 380.
- Lucander, M., Björkqvist, T., *New approach on the fundamental defibration mechanisms in wood grinding*, IMPC 2005, International Mechanical Pulping Conference, Oslo Norway, June 7 - 9 2005, Proceedings p. 149 - 155.
- Tuovinen, O., *Power threshold effect in grinding - an expression of elastic work?* O PAPEL, 2012, 73(5): p. 69 - 73
- Björkqvist, T., *On the Specific Energy Consumption in Mechanical Pulping*, IMPC 2011. International Mechanical Pulping Conference, Xian, China, June 26-29, 2011, Proceedings p. 492-495
- Lucander, M., Asikainen, S., Pöhler, T., Saharinen, E., Björkqvist, T. (2009). *Fatigue treatment of wood by high-frequency cyclic loading*. J Pulp Pap Sci, 35(3-4), 81-85.
- Salmi, A., Salminen, L. I., Engberg, B. A., Björkqvist, T., Hægström, E. (2012a). *Repetitive impact loading causes local plastic deformation in wood*. J. Appl. Phys., 111(2), 024901.
- Salmi, A., Salminen, L. I., Lucander, M., Hægström, E., *Significance of fatigue for mechanical defibration*. Cellulose, 19(2)2012, 575-579.
- Björkqvist T., Lucander M., Tuovinen, O., *Method and device for mechanical separation of wood into fibers*, patent US2006283990
- Tuovinen, O., *Device and Method for Defibration of Wood*, patent US2009308549
- Tuovinen, O., Fardim, P., Lönnberg, B., *An investigation into topographic changes in pulp stone grits and their impact on pulp quality during stabilization process*. Paperi ja Puu, 2008. 90(7): p. 38-43
- Tuovinen, O., Wiinämäki, A., Fardim, P., *Initial fiber effects in pressurized grinding as analyzed by SEM*, IMPC 2009, International Mechanical Pulping Conference, Sundvall, Sweden, May 31 - June 4 2009, Proceedings p. 111 - 116.
- Tuovinen, O., Björkqvist, T., Fardim, P., *Reconstruction and characterization of grinding wheel and grit topography from scanning electron microscopy stereo micrographs with digital photogrammetry*, O PAPEL, 2013. 74(4): p. 51 - 58
- <http://www.sympatec.com/EN/ImageAnalysis/Fundamentals.html>